Hebert, H., Jørgensen, P. L., Skriver, E., & Maunsbach, A. B. (1982) *Biochim. Biophys. Acta 689*, 571–574.
Hegyvary, C., & Jørgensen, P. L. (1981) *J. Biol. Chem. 256*, 6296–6303.
Huang, W. H., Kakar, S. S., & Ascari, A. (1985) *J. Biol. Chem. 260*, 7356–7361.
Jensen, J., & Ottolenghi, P. (1983) *Biochim. Biophys. Acta 731*, 282–289.
Jørgensen, P. L. (1974) *Biochim. Biophys. Acta 356*, 36–52.
Jørgensen, P. L. (1983) in *Structure and Function of Membrane Proteins* (Palmieri et al., Eds.) pp 245–254, Elsevier, Amsterdam.
Jørgensen, P. L., & Karlish, S. J. D. (1980) *Biochim. Biophys. Acta 597*, 305–317.
Jørgensen, P. L., Klodos, I., & Petersen, J. (1978) *Biochim. Biophys. Acta 507*, 8–16.
Karlish, S. J. D. (1980) *J. Bioenerg. Biomembr. 12*, 111–136.
Karlish, S. J. D., & Yates, D. W. (1978) *Biochim. Biophys. Acta 527*, 115–130.
Karlish, S. J. D., & Stein, W. D. (1982) *J. Physiol. (London) 328*, 295–316.
Karlish, S. J. D., Jørgensen, P. L., & Gitler, C. (1977) *Nature (London) 269*, 715–717.
Martin, D. W. (1983) *Biochemistry 22*, 2276–2282.
Martin, D. W., Tanford, C., & Reynolds, J. A. (1984) *Proc. Natl. Acad. Sci. U.S.A. 81*, 6623–6626.
Møller, J. V., Lind, K. E., & Andersen, J. P. (1980) *J. Biol. Chem. 255*, 1912–1920.
Steinberg, M., & George, J. J. D. (1982) *Arch. Biochem. Biophys. 219*, 359–365.
Tanford, C. (1970) *Adv. Protein Chem. 24*, 1–95.
Tanford, C., Nozaki, Y., Reynolds, J. A., & Makino, S. (1974) *Biochemistry 13*, 2369–2376.

Triplet–Singlet Energy Transfer in the Complex of Auramine O with Horse Liver Alcohol Dehydrogenase†

Jeffry G. Weers‡ and August H. Maki*
Department of Chemistry, University of California, Davis, California 95616
Received September 27, 1985; Revised Manuscript Received December 17, 1985

ABSTRACT: Triplet–singlet energy transfer has been studied in the complex formed between auramine O (AO) and horse liver alcohol dehydrogenase with optically detected magnetic resonance (ODMR) spectroscopy. The results show that Trp-15 and Tyr residues transfer triplet energy mainly by a trivial process, whereas Trp-314 transfers triplet energy by a Förster process with two observed lifetimes at 77 K of 170 and 50 ms. The different Förster energy-transfer lifetimes are ascribed either to quenching of the two Trp-314 residues of the dimer by a single asymmetrically bound AO or to two distinct conformations of the enzyme–dye complex with differing separations and/or orientations of donor and acceptor. Individual spin sublevel transfer rate constants are reported for the major decay component with the 170-ms Trp triplet-state lifetime; these are found to be highly selective with $k_x^{tr} \gg k_y^{tr}$ and k_z^{tr}.

The development of chemical modification techniques for proteins has led to important information regarding the structure, function, and dynamics of many proteins (Means & Feeney, 1971). In particular, introduction of fluorophores into protein structures gives the experimentalist a direct probe for obtaining this information (Cantor & Schimmel, 1980; Chen & Edelhoch, 1975). The binding of dyes to globular proteins has received considerable attention [Glazer (1970) and refereces cited therein]. Many dyes have the interesting property of being virtually nonfluorescent in aqueous solution but become highly fluorescent when bound to proteins (Edelman & McClure, 1968; Turner & Brand, 1968; Chen, 1977). In addition to the dramatic change in their radiative quantum yields in various environments, the dye fluorescence maximum exhibits large shifts. Also, denaturation of the protein or the binding of small molecules such as cofactors or substrates can lead to differences in dye properties (Velick, 1961; Weber & Daniel, 1966; Heitz & Brand, 1971). Glazer (1970) has reviewed a number of dye–protein complexes and has shown that the strong binding of dyes to simple globular proteins generally takes place in areas overlapping the binding sites for substrates, coenzymes, or prosthetic groups, in preference to other regions of the protein structure. Thus, dyes are useful probes for investigating protein structure and function near enzyme active sites.

An enzyme–dye complex that has received considerable attention is that formed between the cationic dye auramine O (AO)[1] and the enzyme horse liver alcohol dehydrogenase (HLAD) (Conrad et al., 1970; Sigman & Glazer, 1972; Chen, 1977; Heitz & Brand, 1971). AO has a fluorescence quantum yield of 4×10^{-5} in aqueous solution, which increases over 1000-fold to 5.5×10^{-2} when it is bound to HLAD (Chen, 1977). By monitoring changes in the AO binding and fluorescence properties upon addition of certain active site directed compounds, Heitz and Brand (1971) were able to identify the location of the dye binding site. The dye was found to bind directly adjacent to the active site in a region overlapping the cyclohexanol binding site but not the ethanol binding site.

† This research was supported by a grant from the National Science Foundation.
‡ Present address: Clorox Technical Center, Pleasanton, CA 94566.

[1] Abbreviations: ODMR, optical detection of triplet-state magnetic resonance; AO, auramine O; HLAD, horse liver alcohol dehydrogenase; MIDP(L), microwave-induced delayed phosphorescence (luminescence); Trp, tryptophan; Tyr, tyrosine.

0006-2960/86/0425-2897$01.50/0

In addition to providing information about their immediate environment, another unique feature of bound dyes is their ability to quench the intrinsic luminescence of Trp residues through long-range dipole–dipole energy-transfer processes (Cantor & Schimmel, 1980). The theory for the dipole–dipole model was first developed by Förster (1948, 1965), with the result that in the weak coupling limit the rate constant for energy transfer between an excited donor molecule and an acceptor is given by

$$k^{tr}_i = (8.71 \times 10^{23}) k_i Q_i r_i^{-6} K^2_i J_i n^{-4} \text{ s}^{-1} \quad (1)$$

The subscript i refers to a particular donor state having a total decay constant k_i and radiative quantum yield Q_i in the absence of energy transfer. The product k_iQ_i may be associated with the radiative rate constant k^r_i. r_i is the distance in angstroms separating the transition dipoles of donor and acceptor, while n is the refractive index of the medium separating them. K^2_i is an orientation factor that accounts for the fact that the interaction of two dipoles in space depends upon their relative orientations. J_i is an overlap integral between the donor's emission spectrum, $I_i(\lambda)$, and the absorption spectrum of the acceptor, $\epsilon(\lambda)$, normalized over $I_i(\lambda)$ only and is given by

$$J_i = \int I_i(\lambda)\epsilon(\lambda)\lambda^4 \, d\lambda / \int I_i(\lambda) \, d\lambda \quad (2)$$

There are no restrictions on the multiplicity of the donor and acceptor chromophores, although triplet acceptor states generally lead to small transfer rate constants because of the low value of $\epsilon(\lambda)$ that appears in J_i. For this reason, singlet–singlet and triplet–singlet energy-transfer processes predominate. The magnitude of triplet–singlet transfer rate constants is limited by the small k_i for triplet states. The efficiency of energy transfer, $\text{Eff}_i = k^{tr}_i/(k^{tr}_i + k_i)$, is clearly independent of k_i, however. In other words, triplet–singlet energy-transfer processes occur with the same efficiency and distance dependence (up to ca. 50 Å) as singlet–singlet energy transfer for comparable values of K^2_i, Q_i, and J_i, even though k_i is small.

There are many examples of the measurement of singlet–singlet energy transfer in dye–protein complexes (Conrad et al., 1970; Stryer, 1968; Fairclough & Cantor, 1977). The fluorescence techniques used to study this process have proven useful in obtaining information about the binding of ligands to proteins (Velick, 1961; Weber & Daniel, 1966) and as a ruler for estimating the distance between the dye and Trp molecules within the complex (Stryer, 1968, Conrad et al., 1970).

Conrad et al. (1970) have studied the singlet–singlet energy-transfer processes of the AO/HLAD complex discussed earlier. On the basis of fluorescence excitation spectra, their results show that the singlet–singlet energy-transfer efficiency in the 1:1 AO/HLAD complex is only ca. 0.3 and decreases to ca. 0.2 in the 2:1 complex. HLAD is a symmetrical dimer known to contain two Trp residues in each subunit (Branden et al., 1975). One residue (Trp-15) is solvent-exposed on the surface of the protein and has a ca. 7-ns fluorescence lifetime, while the other (Trp-314) is buried in a hydrophobic region of the protein and has a ca. 4-ns lifetime.

Galley and Stryer (1969) were the first to study triplet–singlet energy transfer for an enzyme–dye complex using the system of proflavin complexed with α-chymotrypsin. They found that triplet–singlet energy transfer could be identified by a decrease in the ratio of Trp phosphorescence to fluorescence and by the appearance of sensitized delayed fluorescence from proflavin. Additional information may be available from triplet–singlet energy transfer compared to singlet–singlet energy transfer because of the triplet-state multiplicity, which leads to three distinct spin sublevels per donor site. The three sublevels generally have different properties including different energies (E_i) due to spin–spin dipolar coupling between the triplet electrons. The spin sublevels also have different decay rate constants, k_i, and radiative rate constants, k^r_i, as well as different intersystem crossing rates, p_i, and steady-state populations, N^0_i, because of selective spin–orbit coupling routes. Differences between steady-state populations and between radiative rate constants and/or radiative quantum yields make possible optical detection of magnetic resonance spectroscopy (ODMR) with phosphorescence detection (Clarke, 1982; Maki, 1984). ODMR measurements on Trp require the use of pumped liquid helium temperatures to suppress spin–lattice relaxation and thereby to produce a state of spin alignment. Because of rapid spin–lattice relaxation at 77 K, the sublevels are strongly coupled and only the average of the sublevel decay constants is obtained. By performing transient ODMR experiments at ca. 1.2 K, however, it is possible to obtain the individual spin sublevel decay constants and from these to deduce the individual energy-transfer rate constants. These are expected to differ between triplet sublevels since it is generally true that $k^r_i \neq k^r_j$. Also, the sublevel orientation factors may differ since their phosphorescences may be polarized differently. Finally, the spectral overlap integrals may not be equal if the phosphorescence from one sublevel is only vibronically allowed while that of another sublevel is allowed electronically, for example.

Maki and Co (1976) studied triplet–singlet energy transfer in the proflavin–chymotrypsin complex using ODMR spectroscopy. The triplet donor species was identified by the observation of Trp microwave-induced slow-passage ODMR signals while the proflavin-delayed fluorescence was being monitored. Although the Trp D + E ODMR signal is difficult to observe normally since this transition couples only very weakly radiative sublevels (Maki & Zuclich, 1975), it was observed easily in the proflavin–chymotrypsin complex when the delayed fluorescence was monitored. This feature demonstrates the enhancement of ODMR signals from weakly radiative sublevels by coupling the triplet state with a fluorescent dye. ODMR signal intensities also may be enhanced as the result of increased spin alignment of the triplet sublevels induced by selective energy transfer to the dye. The kinetics for the proflavin–chymotrypsin system were difficult to analyze due to energy transfer with differing k^{tr} from at least four Trp's.

In this study the triplet–singlet energy-transfer processes in the AO–HLAD complex are examined by ODMR spectroscopy. Because HLAD contains only two Trp residues (Trp-15 and Trp-314) that are resolvable both in their phosphorescence spectra (Purkey & Galley, 1970) and in their ODMR spectra (Zuclich et al., 1973; Ross et al., 1980), it is possible to study each Trp selectively, and it also is possible, in principle, to measure individual spin sublevel transfer rate constants by monitoring the delayed fluorescence at pumped liquid helium temperatures where spin–lattice relaxation is quenched. This work provides direct evidence for the participation of both Trp residues in the triplet–singlet energy-transfer process. Although Trp-314 transfers energy to AO via the Förster mechanism, triplet–singlet energy transfer from Trp-15 occurs by a trivial process, demonstrating the weakness of the coupling between this residue and AO.

Materials and Methods

AO and HLAD were purchased from Sigma. AO was

purified by recrystallization from water in the dark. The lyophilized enzyme was dissolved in 100 mM potassium phosphate buffer (pH 7.4), and it was subsequently dialyzed against this buffer. Complexes with AO were formed by equilibrium dialysis over a 24-h period in the same buffer as described above. Sample concentrations were determined by absorbance spectroscopy with extinction coefficients obtained previously [$\epsilon_{280} = 3.54 \times 10^4$ M^{-1} cm^{-1} for HLAD (Sund & Theorell, 1963) and $\epsilon_{430} = 4.41 \times 10^4$ M^{-1} cm^{-1} for AO (Conrad et al., 1970)]. For the 1:1 sample, the concentrations used were 1.5×10^{-4} M for both HLAD and AO, while for the 2:1 sample the concentrations of AO and HLAD were 1.8×10^{-4} and 9.2×10^{-5} M, respectively. For low-temperature spectroscopic measurements, 20% (v/v) glycerol (Aldrich Gold Label) was added. Luminescence measurements were made at 77 K. To eliminate the immediate fluorescence background, a rotating can sector with a dead time of ca. 1 ms was used. The sample was optically pumped with a 100-W high-pressure Hg arc lamp fitted in a Photochemical Research Associates (Model ALH-215) housing. The exciting light was passed through a $NiSO_4$ solution filter and a 10-cm monochromator (Instruments SA H-10) and then focused onto the sample. The emission was viewed at right angles through a WG-345-2 glass filter and a 1-m monochromator (McPherson Model 2051), and it was detected with a photomultiplier tube (EMI 9789QA). Luminescence decay measurements were performed in a manner described previously (Maki & Co, 1976). The decays were averaged on a Nicolet (Model 1072) signal averager, and kinetic analysis was carried out on a Digital Equipment Corp. Professional-350 microcomputer. A curve-peeling technique was used initially in which plots of the logarithm of the intensity vs. time were displayed on the monitor. The tail of the plot was then fitted to a straight line. The computer subsequently subtracted the fit and displayed the difference. This process was repeated until no significant intensity, outside of the noise, remained in the difference plot. The preexponentials and decay constants obtained from this analysis were then used as initial guesses in a Marquardt algorithm (Bevington, 1969). Plots of residuals were considered satisfactory when the deviation was ±5% or less. ODMR slow-passage and microwave-induced delayed luminescence (MIDL) experiments were performed at ca. 1.2 K. The slow-passage frequencies were obtained with 30-s sweep times, and the values that we report are the average of responses obtained when sweeping in each direction to minimize fast-passage effects. The sector was used during slow-passage measurements to remove unwanted nonsensitized AO fluorescence background. MIDL experiments were performed in a manner described previously for phosphorescence detection, MIDP (Schmidt et al., 1971). The individual decay constants for the long-lived sublevels, T_y and T_z, were obtained with a linear regression fit to plots of ln h_{xj} vs. t', where h_{xj} ($j = y$ and z) is the height of the MIDL response to the $T_x \leftrightarrow T_j$ transition at delay time t'. The slope of the line yields the decay constant k_j. The correlation coefficient obtained for the linear fit was greater than 0.98 in each case. The decay constant k_x for the T_x sublevel was obtained by a deconvolution of the decay of the MIDL response transient.

Results

Luminescence Spectra. The phosphorescence spectrum for HLAD (Figure 1) is a superposition of two Trp spectra whose origins are shifted from each other by ca. 6 nm (Purkey & Galley, 1970). This leads to two optically resolved 0,0 bands at 406.0 and 411.8 nm. The blue-shifted emission is due to residues in a polar medium exposed to the solvent and has been assigned to Trp-15, while the red-shifted emission is due to Trp-314, which is shielded from the solvent in a more polarizable region of the protein. The spectrum obtained for HLAD with 280-nm excitation (Figure 1B) shows a large contribution from both Trp-15 and Trp-314, as well as a noticeable contribution from Tyr below 400 nm. Moving the excitation wavelength to 300 nm (Figure 1A) results in a dramatic decrease in the phosphorescence intensity of Trp-15 and Tyr. Both of these spectra were obtained with a 16-nm excitation band-pass. If one moves the excitation peak to 305 nm and narrows the band-pass to 4 nm, it is possible to obtain phosphorescence from Trp-314 only (Purkey & Galley, 1970). There is a dramatic change in the delayed luminescence spectrum after binding the dye to the enzyme (Figure 2). The Trp phosphorescence of Figure 1 is almost completely quenched, with only a small residual amount observable between 400 and 450 nm. The luminescence at $\lambda > 450$ nm is a combination of delayed fluorescence ($\lambda_{max} = 486$ nm) from AO that we think results from triplet–singlet energy-transfer processes and AO phosphorescence ($\lambda_{max} = 535$ nm) that may result from direct excitation of the dye, as well as from intersystem crossing following energy transfer. The relative contribution of AO phosphorescence to the delayed luminescence is much less when 280-nm excitation (Figure 2A) is used than when 305-nm excitation is used (Figure 2B), since AO absorbs more strongly at the longer wavelength.

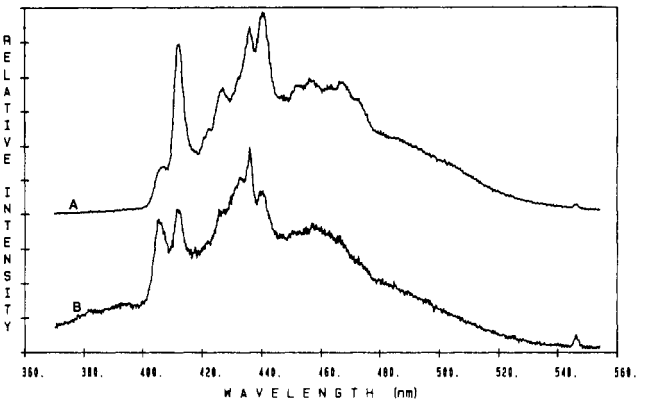

FIGURE 1: Phosphorescence spectra at 77 K for 2×10^{-3} M HLAD in 20% glycerol–buffer. (A) Sample is excited at 300 nm with a 16-nm excitation band-pass, and emission is scanned with a 1.5-nm band-pass. (B) Sample is excited at 280 nm with a 16-nm excitation band-pass, and emission is scanned with a 1.5-nm band-pass.

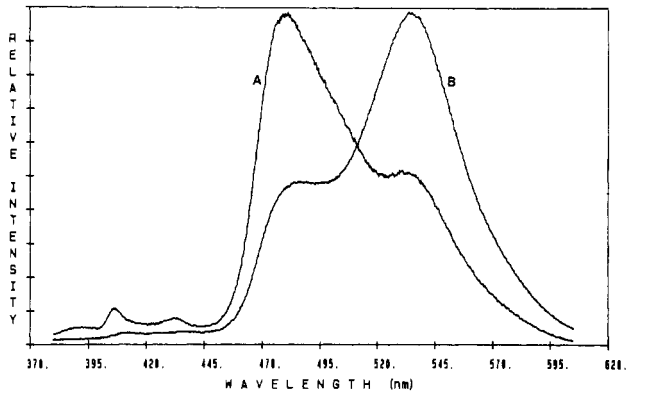

FIGURE 2: Delayed luminescence spectra at 77 K for the 2:1 AO/HLAD complex in 20% glycerol–buffer solution. The spectra are obtained with the rotating sector, which effectively eliminates all background luminescence with a lifetime less than ca. 1 ms. (A) The sample is excited at 280 nm with a 4-nm excitation band-pass, and the emission is scanned with a 3-nm band-pass. (B) The sample is excited at 305 nm with a 4-nm excitation band-pass, and the emission is scanned with a 3-nm band-pass.

Table I: Decay Analyses for AO/HLAD Samples[a]

sample	λ_{exc} (nm)	λ_{obsd} (nm)	dwell (ms/ch)[b]	preexp (%)	lifetime (s)	assignment
HLAD	305	412	33	100	5.59	unperturbed Trp
AO	305	545	6.6	100	1.37	AO phosphorescence
2:1 sample	305	545	6.6	100	1.41	AO phosphorescence
1:1 sample	305	494	22	16.8	5.29	trivial-transfer Trp-314
				15.6	1.0	AO phosphorescence
				67.6	0.15	Förster-transfer Trp-314
1:1 sample	305	494	1.1	15.0	1.4	AO phosphorescence
				56.2	0.17	Förster-transfer Trp-314
				28.8	0.05	Förster-transfer Trp-314
2:1 sample	305	494	1.1	15.8	1.0	AO phosphorescence
				56.8	0.17	Förster-transfer Trp-314
				27.5	0.05	Förster-transfer Trp-314
2:1 sample	305	494	22	*c*	*c*	no 5-s component observed
1:1 sample	280	494	22	46.5	5.59	trivial-transfer Trp-15
				19.7	1.72	trivial-transfer Tyr or Förster-transfer Trp-15
				33.8	0.20	Förster-transfer Trp-314
1:1 sample	280	494	1.1	40.3	2.4	trivial-transfer Trp-15, Tyr
				38.3	0.17	Förster-transfer Trp-314
				21.4	0.04	Förster-transfer Trp-314
2:1 sample	280	494	1.1	31.9	1.7	trivial-transfer Trp-15, Tyr
				41.9	0.17	Förster-transfer Trp-314
				26.2	0.04	Förster-transfer Trp-314
2:1 sample	280	494	22	34.8	5.17	trivial-transfer Trp-15
				20.3	2.03	trivial-transfer-Tyr or Förster-transfer Trp-15
				44.9	0.36	Förster-transfer Trp-314

[a] T = 77 K, and all studies of AO/HLAD samples were performed with 4-nm excitation slit widths and 3-nm emission slit widths. [b] The decay is followed for ca. 1000 channels. [c] No long-lived components are observed. Luminescence decays to base line in ca. 700 channels.

Decay Analysis at 77 K. The decay data obtained at 77 K for the AO/HLAD complex that is presented in Table I are quite complicated due to the emission from multiple chromophores, as well as the existence of Förster and trivial triplet–singlet energy-transfer processes. For this reason, two decays were obtained and analyzed for each excitation and emission wavelength. The first (dwell time = 22 ms/channel) emphasizes the long-lived components, while the second (dwell time = 1.1 ms/channel) emphasizes the short-lived components. When 305-nm excitation with a 4-nm band-pass is used, only Trp-314 and AO are excited. Delayed AO fluorescence due to triplet–singlet energy transfer from Trp-314 and AO phosphorescence contribute to the luminescence decay when the delayed luminescence at 494 nm is monitored. Residual Trp and Tyr phosphorescence make a negligible contribution under these conditions (Figure 2B). When the decay of the 1:1 sample is measured with a 22 ms/channel dwell time, a triexponential is obtained, 5.29 s (16.8%), 1.0 s (15.6%), and 150 ms (67.6%). The 5.29-s component has a lifetime similar to that of uncomplexed HLAD and is attributed to trivial energy transfer in which an emitted Trp photon is absorbed by AO and is subsequently reemitted as delayed fluorescence. The source of this component is HLAD molecules that are not complexed with AO. The intensity of this component is too large to be accounted for by direct Trp phosphorescence. The 1.0-s component probably is due to underlying AO phosphorescence although the value is somewhat less than the 1.4-s lifetime that is found in uncomplexed AO. The 150-ms component that dominates the decay is assigned to AO-delayed fluorescence resulting from Förster energy transfer from Trp-314. Measurements made with the 1.1 ms/channel dwell time emphasize the short-decay components. Under these conditions, we find a 1.4-s component due to AO phosphorescence as well as 170- and 50-ms lifetimes, which we assign to Förster transfer from Trp-314. In the 2:1 sample, the results we find using the 1.1 ms/channel dwell time are nearly identical with those obtained in the 1:1 sample. Using a 22 ms/channel dwell time, it is impossible for us to observe a 5-s component, which implies that the contribution of trivial energy transfer is very small for the 2:1 sample.

When 280-nm excitation is used, both Trp-15 and Trp-314 are photoexcited. In addition, Tyr contributes to the decay. At this excitation wavelength, the contributions of AO phosphorescence as well as that of Trp and Tyr at the observation wavelength of 494 nm are negligible (Figure 2A). For the 1:1 sample with a 22 ms/channel dwell time, we obtain the components 5.59 s (46.5%), 1.72 s (19.7%), and 200 ms (33.8%). The 200-ms component is assigned to Förster transfer from Trp-314, which we observed previously using 305-nm excitation. The large amplitude of the 5.6-s delayed fluorescence component, assigned principally to energy transfer from Trp-15, demonstrates that this residue decays predominantly by trivial processes. The 1.72-s component is due either to trivial energy transfer from Tyr or Förster energy transfer from Trp-15. With the short dwell time of 1.1 ms/channel, 170- and 40-ms components from Trp-314 Förster transfer are found to dominate the decay. There also is an apparent 2.4-s component, which is assigned to an unresolved combination of the 5.6- and 1.7-s components obtained with the long dwell time. In the 2:1 sample, the amplitudes of the short Trp-314 Förster components are enhanced, and a smaller contribution of the 5-s component assigned to trivial triplet–singlet energy transfer is observed. This points to a decrease in the amount of trivial triplet–singlet energy transfer from Trp-314, which is consistent with the results obtained with 305-nm excitation.

In summary, the decay analysis of the AO delayed luminescence indicates predominantly trivial triplet–singlet energy transfer from Trp-15, while Förster triplet–singlet energy transfer is found to occur from Trp-314, resulting in reduced average lifetimes of 170 and 50 ms. Trivial energy transfer from Tyr also occurs and is supported by ODMR results to be presented below.

Slow-Passage ODMR. The 1.2 K slow-passage ODMR data are presented in Table II. The residual Trp phosphorescence contributing to the delayed luminescence of the enzyme–dye complex at 494 nm constitutes no more than ca. 3% of the total intensity. Therefore, the observation of Trp slow-passage signals at this wavelength must be the result of Trp's role as a donor in triplet–singlet energy-transfer pro-

Table II: Slow Passage ODMR Results

sample	λ_{exc} (nm)	λ_{obsd} (nm)	2E (GHz)	D – E (GHz)	D + E (GHz)	assignment
HLAD[a]	280	406	2.544	1.770		Trp-15
	305	412	2.544	1.660		Trp-314
apoazurin[b]	280	383	3.40	2.19	5.59	Tyr
1:1 AO/HLAD sample	280	494	2.52	1.74		Trp-15
	280	494	~4[c]		5.5	Tyr
	305	494	2.52	1.68		Trp-314

[a] ODMR results taken from Ross et al. (1980). [b] ODMR results taken from Ugurbil et al. (1977). [c] Accurate determination of frequency was not possible beause it occurs between two octaves of the microwave sweeper plug-in units. This signal and the one obtained at 5.5 GHz could not be observed with 305-nm excitation.

Table III: Microwave-Induced Delayed Luminescence Measurements

sample	λ_{exc} (nm)	λ_{obsd} (nm)	k_x (s^{-1})[a]	k_y (s^{-1})[a]	k_z (s^{-1})[a]	k^r_x (s^{-1})	k^r_y (s^{-1})	k^r_z (s^{-1})
HLAD	280	405	0.32	0.082	0.050			
	305	412	0.36	0.088	0.055	0.36[b]	0.041[b]	0.025[b]
2:1 AO/HLAD sample	305	494	16.6	1.9	1.13			

[a] The decay constants were obtained from MIDP and MIDL measurements and were not corrected for the effects of spin–lattice relaxation. See text. T = 1.21 K. [b] Radiative rate constants were determined from MIDP analysis of the 2:1 AO/HLAD sample with $k^{tr} \propto k^r C$. The constant C was determined for the T_x sublevel with $Q_x = 1$ and was assumed to be the same for T_y and T_z.

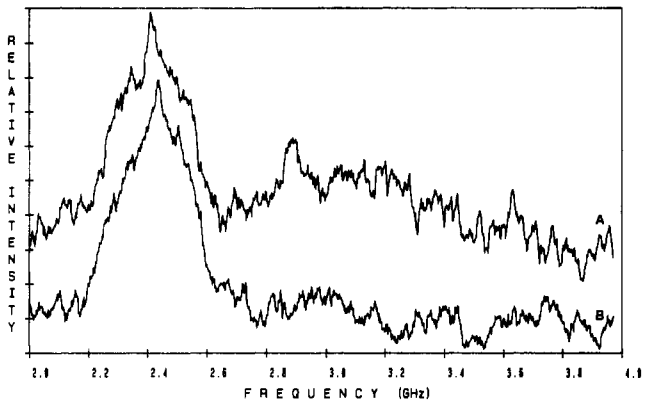

FIGURE 3: Slow-passage ODMR spectra of the Trp 2E signal, for the 1:1 AO/HLAD sample at 1.2 K. Spectra were obtained by monitoring the delayed fluorescence at 494 nm, with excitation at (A) 305 nm and (B) 280 nm. The microwaves are swept from 4 to 2 GHz in 30 s; the signals obtained are the result of 64 accumulations.

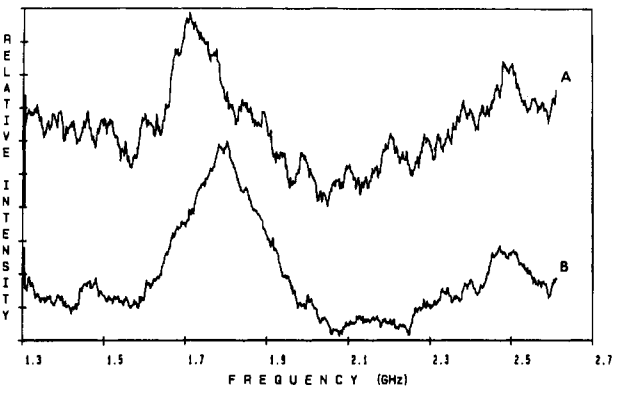

FIGURE 4: Slow-passage ODMR spectra of the Trp D – E signal, for the 1:1 AO/HLAD sample at 1.2 K. Spectra were obtained by monitoring the delayed fluorescence at 494 nm, with excitation at (A) 305 nm and (B) at 280 nm. The microwaves are swept from 1.4 to 2.5 GHz in 30 s; the signals obtained are the result of 64 accumulations.

cesses. Figures 3 and 4 show the Trp 2E and D – E slow-passage signals of the enzyme–dye complex obtained with 280- and 305-nm excitation while the delayed fluorescence was monitored. The frequencies obtained with 30-s microwave sweep times are very close to those previously obtained for HLAD by Ross et al. (1980). The shift in frequency of the D – E transition between Trp-15 and Trp-314 makes it possible to distinguish between the two residues. The frequency shift of the D – E signal that is observed between the two spectra for the 1:1 AO/HLAD sample with 280- and 305-nm excitation indicates the involvement of both Trp's in a triplet–singlet energy-transfer process. With 305-nm excitation, the Trp ODMR signals obtained when the AO delayed fluorescence is monitored should originate from Trp-314. The ODMR frequencies are in good agreement with those observed for this residue when the phosphorescence of HLAD at 412 nm (Table II) is monitored. With 280-nm excitation, the ODMR frequencies shift into good agreement with those observed for the Trp-15 residues of HLAD, indicative that this residue participates in energy transfer to AO. With a shorter 10-s sweep time, there is a definite fast-passage transient contribution to the ODMR transitions when 280-nm excitation is used, which is a further indication that Trp-15 transfers its excitation in a trivial manner. Two signals are obtained at higher frequencies with 280-nm excitation. The first is a negative signal near ca. 4 GHz. Because the signal lies in a region overlapping two octaves of the BWO microwave sweeper plug-in units, it is impossible to obtain an accurate frequency. Another signal is observed at ca. 5.5 GHz. This is in the same frequency region as the D + E transition obtained previously for Tyr (Ugurbil et al., 1977). Since the amino acid phosphorescence at this wavelength is negligible, the assignment of this signal to Tyr illustrates the involvement of this amino acid in triplet–singlet energy-transfer processes. The response near 4 GHz may be due either to the D+E signal of Trp, to the 2E signal of Tyr, or to a combination of the two. Shifting the excitation to 305 nm where neither Tyr nor Trp-15 absorbs results in the loss of both signals, indicating that neither one is due to Trp-314.

Microwave-Induced Delayed Luminescence Measurements. Since it appears that Trp-314 decays predominantly by Förster processes in the 2:1 sample, we attempted to obtain individual triplet spin sublevel lifetimes influenced by energy transfer by monitoring the delayed fluorescence at sufficiently low temperatures that the sublevels are decoupled from one another. The technique employed for this measurement is MIDL, which is analogous to the MIDP experiment (Schmidt et al., 1971). Since there are two Förster lifetime components for Trp-314 (170 and 50 ms), the question arises as to which component we are studying using the MIDL technique. When an excitation period as long as 1 s is used, we selectively enhance the decay of the longer 170-ms component observed at 77 K.

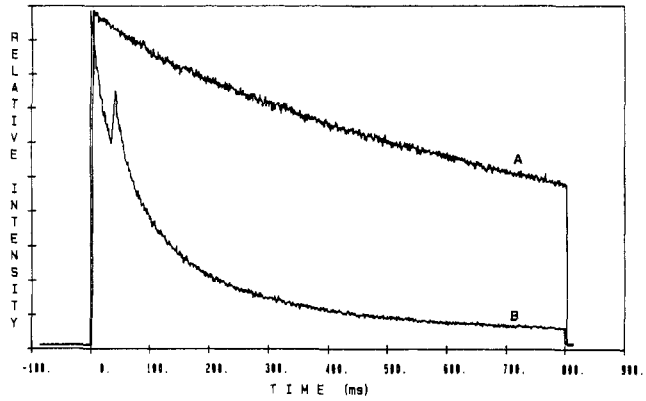

FIGURE 5: MIDL spectra for the 2:1 AO/HLAD sample at 1.2 K with a 305-nm excitation pulse of 1-s duration. Microwaves are swept through the Trp D – E transition in ca. 2 ms with 50 mW of microwave power at $t' = 50$ ms. The decays are accumulated over 512 scans. (A) The AO phosphorescence is monitored at 545 nm. (B) The AO delayed fluorescence is monitored at 494 nm.

Hence, the contribution of the 50-ms component is small. With anticipation of the results, the average delayed fluorescence lifetime obtained for the complex from the MIDL analysis is 153 ms, which agrees well with the 170-ms lifetime component obtained from the decay analysis at 77 K. The results obtained are given in Table III. For comparison, we obtained also the apparent (not corrected for spin–lattice relaxation) individual spin sublevel decay constants for both Trp's in uncomplexed HLAD using the MIDP technique. In order to prove that the MIDP signals obtained in the AO/HLAD complex were indeed from Trp and not from the triplet state of AO, we also looked selectively for a MIDL response while monitoring the AO phosphorescence under the same conditions. No signal was obtained (Figure 5A), which shows that the MIDL response in Figure 5B definitely is due to Trp. Although strong MIDL response were obtained for the D – E and 2E transitions of Trp, no signal was obtained in the D + E region. This seems to indicate either that the T_y and T_z sublevels have nearly the same energy-transfer rate constants or that their steady-state populations are nearly equal. The MIDL results show that all three sublevels of Trp-314 are affected dramatically by the energy-transfer process. The decay rate constant k_x increases by a factor of 46, while k_y and k_z increase by factors of approximately 22 and 21, respectively, when HLAD is complexed with AO.

Discussion

The room temperature association constant of the two independent AO binding sites in HLAD is 1×10^5 M^{-1} (Conrad et al., 1970). A simple calculation shows that for a 1:1 AO/HLAD ratio sample at a concentration of 10^{-4} M ca. 30% of the dye is unbound at room temperature. For the 2:1 AO/HLAD ratio sample only ca. 4% of the HLAD molecules contain no bound AO. Our sample freezes at about −8 °C (Douzou, 1977) where the association could be somewhat larger. Considerable amounts of free AO, as well as AO-free enzyme molecules, however, would still be expected, especially in the 1:1 sample. HLAD can use a variety of alcohols as substrates (Sund & Theorell, 1963; Holzer et al., 1955), and many of these have been shown to be competitive inhibitors of AO binding (Conrad et al., 1970; Heitz & Brand, 1971; Sigman & Glazer, 1972). Our samples contain 20% glycerol as a cryosolvent, but the effect of glycerol on AO binding has not been studied. It is clear from the kinetics, however, that there is a complex formed between AO and HLAD and that considerable amounts of AO must be bound, especially in the 2:1 sample. Otherwise, there would be no short AO-delayed luminescence components, which can result only from triplet–singlet energy transfer by a Förster mechanism to bound AO molecules. Also, we would expect that there would be a strong 5-s component due to trivial energy transfer from Trp-314, if there were a significant fraction of HLAD molecules without any bound AO. Although a minor 5-s component is observed with the 1:1 dye/enzyme ratio under 305-nm excitation, none is observed with a 2:1 ratio. Whether or not the AO binding sites are the same as in the absence of glycerol is not absolutely certain, although dyes tend to be very selective in their binding properties to enzymes (Glazer, 1970).

There are two Förster components observed in the decay of the delayed fluorescence with 305-nm excitation. This implies that there are two distinct energy-transfer rate constants for Trp-314. One possible explanation is cross quenching of Trp-314 in one subunit by AO molecules in both subunits, leading to a shorter triplet-state lifetime. This is reasonable, since there could be significant HLAD molecules with both one and two AO's bound. When the relative concentration of AO is increased, however, we would expect a corresponding increase in the relative amplitude of the shorter 50-ms component. In fact, the two Förster components have about the same relative amplitude in both the 1:1 and 2:1 samples. This result is inconsistent with this cross-quenching mechanism. A second possibility is that the two lifetimes correspond to quenching of the two Trp-314 sites of the dimer by a single bound AO. In this case, the insensitivity of the decay lifetimes and amplitudes to the HLAD/AO ratio implies that binding is restricted to one site per dimer, possibly the result of interactions with the cryosolvent. A third possibility is that the AO/HLAD complex is frozen in two distinct conformations whose values of K^2_i and r_i for Trp-314 may differ somewhat. The transfer rate constant could be extremely sensitive to such conformational changes unlike the normal phosphorescence lifetime, which is known to be relatively insensitive to such effects (Longworth, 1971). This explanation has been used to explain multiple fluorescence lifetimes observed in human hemoglobin (Szabo et al., 1984). The insensitivity of the amplitudes and values of the two Förster components to the HLAD/AO ratio is not readily explained, however. It is possible to estimate the distances between Trp-314 and the bound AO with eq 1. J was calculated from eq 2 with Simpson's rule to yield $J = 1.0 \times 10^{-13}$ cm^6/mmol, $n = 1.4$ for the glycerol–buffer cosolvent system, $K^2 = 0.475$ in rigid random matrices (Maksimov & Rozman, 1962; Steinberg, 1968), and $k^r = (1/3)k_x = 0.12$ s^{-1}, assuming that T_x is the only radiative sublevel in Trp and that $Q_x \approx 1$ (Maki & Zuclich, 1975). From this one obtains distances of ca. 25 and 20 Å, which correspond to the 170- and 50-ms components, respectively. These estimates compare favorably with the 19-Å distance obtained by X-ray methods (Eklund et al., 1976) for the intramonomer spacing between Trp-314 and the active site. AO is known to bind in a region overlapping the active site (Heitz & Brand, 1971). Since the distance between the two Trp-314 in the dimer is ca. 5 Å, our results appear to be in accord with direct and cross quenching by a single bound AO, corresponding to the second model discussed above. A large source of uncertainty in these estimates is the value of K^2. Differences in this quantity may contribute significantly to the different transfer rate constants of the Trp's, rather than differences in the donor–acceptor distance. However, the agreement is still quite good.

The weakness of the D + E slow-passage ODMR signal in HLAD has been ascribed to the near equivalence of the ra-

diative quantum yields for the T_y and T_z sublevels. The individual radiative rate constants and quantum yields for the Trp-314 sublevels in the absence of energy transfer may be estimated from the MIDL analysis of the AO/HLAD complex. There is evidence that the T_x sublevel decay is dominated by radiative processes (Maki & Zuclich, 1975). Thus, in the absence of energy transfer, $k^r_x = k_x = 0.36\ s^{-1}$. Förster energy transfer enhances the decay constant by the terms given in eq 1. These terms can be lumped together as a proportionality constant C, such that $k^{tr}_x = C\,k^r_x$. Solving yields $C = 45.4$. If one assumes that C is the same for each of the triplet sublevels, it is possible to calculate k^r_y and k^r_z from the experimentally measured k^{tr}_y and k^{tr}_z. This assumption requires that J_i and K^2_i are independent of the sublevel i. These assumptions give $k^r_y = 0.041\ s^{-1}$ and $k^r_z = 0.024\ s^{-1}$. The radiative quantum yields are then calculated by dividing the radiative rate constants by the apparent decay rate constants in the absence of transfer (Table III), with the result that $Q_y = 0.47$ and $Q_z = 0.44$. We note that for HLAD itself the total decay constants are probably not very accurate since no correction for spin–lattice relaxation was made in their determination. We conclude, however, that the lack of a D + E slow-passage signal for Trp-314 in HLAD (and in other Trp-containing peptides) may be attributed to the near equivalence of the radiative quantum yields.

The steady-state ODMR signal intensity for the $T_i \leftrightarrow T_j$ transition with phosphorescence detection is given by (Maki, 1984)

$$\Delta P^{ij} = a k_i k_j k_{ij}^{-1}(Q_i - Q_j)(N^0_j - N^0_i) \qquad (3)$$

where a is a constant that depends upon the apparatus, $k_{ij} = (k_i + k_j)$, and Q_i is the quantum yield of T_i phosphorescence; $Q_i = k^r_i/k_i$. If the ODMR transition is observed by monitoring the delayed fluorescence of an acceptor dye molecule, eq 3 is modified by substituting $(k^{tr}_i Q_F)/k_i$ for Q_i, where Q_F is the fluorescence quantum yield of the dye. The change in delayed fluorescence can then be written:

$$\Delta F^{ij} = a' Q_F k_i k_j k_{ij}^{-1}(N^0_j - N^0_i)(k^{tr}_i/k_i - k^{tr}_j/k_j) \qquad (4)$$

Using the data in Table III for Trp-314 in the AO/HLAD complex, the last parenthesized group in eq 4 is only ca. 6×10^{-3} for the $T_y \leftrightarrow T_z$ transition, whereas it increases to $(2–3) \times 10^{-2}$ for the $T_x \leftrightarrow T_y$ and $T_x \leftrightarrow T_z$ transitions. In the case of Trp-314 in the AO/HLAD complex, the k's are sufficiently large that effects due to spin–lattice relaxation (Zuclich et al., 1974) can be ignored without serious error. Furthermore, since $N^0_x \ll N^0_y \approx N^0_z$ due to selective energy transfer from T_x, the other parenthesized group in eq 4 is far larger for the $T_x \leftrightarrow T_y$ and $T_x \leftrightarrow T_z$ transitions than it is for the $T_y \leftrightarrow T_z$ transition. Thus, it is not suprising that we can observe only the transitions involving T_x when monitoring the AO-delayed fluorescence sensitized by energy transfer from Trp-314. On the other hand, we find that in the proflavin–chymotrypsin complex, the $T_y \leftrightarrow T_z$ transition of Trp is readily observed when monitoring the proflavin-delayed fluorescence (Maki & Co, 1976). Thus, for at least one of the coupled Trp's in α-chymotrypsin, k^{tr}_y/k_y and k^{tr}_z/k_z must be quite different.

The results of Conrad et al. (1970) on fluorescence quenching of HLAD by AO showed that the efficiency is rather low (ca. 0.3 or less). Thus, a considerable triplet yield is expected even for Trp-314 in the complex, which is consistent with our observation of triplet–singlet energy transfer from this residue to AO by a Förster process. We find that the triplet state of Trp-15 is not efficiently coupled to AO and that triplet–singlet energy transfer from this residue occurs predominantly by a trivial process. This is effectively supported by the decay analyses of the delayed fluorescence with 280-nm excitation, as well as by the slow-passage ODMR data where fast-passage effects are observed with 10-s sweep times. The ODMR slow-passage and delayed fluorescence decay analysis results show also that Tyr residues undergo triplet–singlet energy transfer by a trivial process. It is interesting that the quenching of the Trp-314 triplet state appears to be quite nearly the same for the 2:1 as it is for the 1:1 AO/HLAD ratio sample. The two transfer rate constants for Trp-314 that we observe cannot be assigned to 2:1 and 1:1 complexes, but we think that they may arise, as discussed earlier, either from energy transfer from the two Trp-314 residues of the dimer to a single asymmetrically bound AO or in some manner from distinct conformations of the enzyme–dye complex. Our results imply that the triplet states of both of the Trp-314 residues in the dimer are quenched by a single bound AO, i.e., that cross quenching occurs efficiently.

ACKNOWLEDGMENTS

We thank J. R. Knutson, D. G. Walbridge, and L. Brand for enlightening discussions of their singlet lifetime measurements on the AO/HLAD complex.

Registry No. L-Trp, 73-22-3; L-Tyr, 60-18-4.

REFERENCES

Bevington, P. R. (1969) *Data Reduction and Error Analysis for the Physical Sciences*, McGraw-Hill, New York.

Branden, C.-I., Jornvall, H., Eklund, H., & Furugren, B. (1975) *Enzymes (3rd Ed.) 11*, 103–190.

Cantor, C. R., & Schimmel, P. R. (1980) *Biophysical Chemistry*, Vol 2, W. H. Freeman, San Francisco.

Chen, R. F. (1977) *Arch. Biochem. Biophys. 179*, 672–681.

Chen, R. F., & Edelhoch, H. (1975) *Biochemical Fluorescence*, Marcel Dekker, New York.

Clarke, R. H. (1982) *Triplet State ODMR Spectroscopy: Techniques and Applications to Biophysical Systems*, Wiley-Interscience, New York.

Conrad, R. H., Heitz, J. R., & Brand, L. (1970) *Biochemistry 9*, 1540–1546.

Douzou, P. (1977) *Cryobiochemistry: An Introduction*, Academic, New York.

Edelman, G. M., & McClure, W. O. (1968) *Acc. Chem. Res. 1*, 65–70.

Eklund, H., Nordstrom, B., Zeppenzauer, E., Soderland, G., Ohlsson, I., Boiwe, T., Soderberg, B. O., Tapia., O., Branden, C. I., & Akeson, A. (1976) *J. Mol. Biol. 102*, 27–59.

Fairclough, R., & Cantor, C. R. (1977) *Methods Enzymol. 48*, 347.

Förster, T. (1948) *Ann. Phys. (Leipzig) 2*, 55.

Förster, T. (1965) in *Modern Quantum Chemistry, Istanbul Lectures* (Sinanoglu, O., Ed.) Part III, p 93, Academic, New York.

Galley, W. C., & Stryer, L. (1969) *Biochemistry 8*, 1831–1838.

Glazer, A. N. (1970) *Proc. Natl. Acad. Sci. U.S.A. 65*, 1057–1063.

Heitz, J. R., & Brand, L. (1971) *Biochemistry 10*, 2695–2700.

Holzer, H., Goedde, H. W., & Schneider, S. (1955) *Biochem. Z. 327*, 245–254.

Longworth, J. W. (1971) in *Excited States of Proteins and Nucleic Acids* (Steiner, R. F., & Weinryb, I., Eds.) pp 319–484, Plenum, New York.

Maki, A. H. (1984) *Biol. Magn. Reson. 6*, 187–294.

Maki, A. H., & Zuclich, J. (1975) *Top. Curr. Chem. 54*, 115–163.

Maki, A. H., & Co, T. (1976) *Biochemistry 15*, 1229-1235.
Maksimov, M. Z., & Rozman, I. M. (1962) *Opt. Spectrosc. (Engl. Transl.) 12*, 337; *Opt. Spektrosk. 12*, 606-609.
Means, G. E., & Feeney, R. E. (1971) *Chemical Modifications of Proteins*, Holden-Day, San Francisco.
Purkey, R. M., & Galley, W. C. (1970) *Biochemistry 9*, 3569-3575.
Ross, J. B., Rousslang, K. W., & Kwiram, A. L. (1980) *Biochemistry 19*, 876-882.
Schmidt, J., Antheunis, D. A., & van der Waals, J. H. (1971) *Mol. Phys. 22*, 1-17.
Sigman, D. S., & Glazer, A. N. (1972) *J. Biol. Chem. 247*, 334-341.
Steinberg, I. Z. (1968) *J. Chem. Phys. 48*, 2411-2415.
Stryer, L. (1968) *Science (Washington, D.C.) 162*, 526-533.
Sund, H., & Theorell, H. (1963) *Enzymes, 2nd Ed. 7*, 25-67.
Szabo, A. G., Krajcorski, D., & Zuker, M. (1984) *Chem. Phys. Lett. 108*, 145-149.
Turner, D. C., & Brand, L. (1968) *Biochemistry 7*, 3381-3390.
Ugurbil, K., Maki, A. H., & Bersohn, R. (1977) *Biochemistry 16*, 901-907.
Velick, S. F. (1961) in *Light and Life* (McElroy, W. D., & Glass, B., Eds.) pp 108-142, Johns Hopkins, Baltimore, MD.
Weber, G., & Daniel, E. (1966) *Biochemistry 5*, 1900-1907.
Zuclich, J., Schweitzer, D., & Maki, A. H. (1973) *Photochem. Photobiol. 18*, 161-168.
Zuclich, J., von Schütz, J. U., & Maki, A. H. (1974) *Mol. Phys. 28*, 33-47.

Apocytochrome *c* Binding to Negatively Charged Lipid Dispersions Studied by Spin-Label Electron Spin Resonance†

Heiner Görrissen‡ and Derek Marsh*
Max-Planck-Institut für biophysikalische Chemie, Abteilung Spektroskopie, D-3400 Göttingen, Federal Republic of Germany
Annie Rietveld and Ben de Kruijff
Laboratory of Biochemistry and Institute of Molecular Biology, State University of Utrecht, Utrecht, The Netherlands
Received October 10, 1985; Revised Manuscript Received January 21, 1986

ABSTRACT: The interaction of apocytochrome *c* with aqueous dispersions of phosphatidylserine from bovine spinal cord and with other negatively charged phospholipids has been studied as a function of pH and salt concentration by using spin-label electron spin resonance (ESR) spectroscopy and chemical binding assays. The ESR spectra of phospholipids spin-labeled at different positions on the *sn*-2 chain indicate a generalized decrease in mobility of the lipids, while the characteristic flexibility gradient toward the terminal methyl end of the chain is maintained, on binding of apocytochrome *c* to phosphatidylserine dispersions. This perturbation of the bulk lipid mobility or ordering is considerably greater than that observed on binding of cytochrome *c*. In addition, a second, more motionally restricted, lipid component is observed with lipids labeled close to the terminal methyl ends of the chains. This second component is not observed on binding of cytochrome *c* and can be taken as direct evidence for penetration of apocytochrome *c* into the lipid bilayer. It is less strongly motionally restricted than similar spectral components observed with integral membrane proteins and displays a steep flexibility gradient. The proportion of this second component increases with increasing protein-to-lipid ratio, but the stoichiometry per protein bound decreases from 4.5 lipids per 12 000-dalton protein at low protein contents to 2 lipids per protein at saturating amounts of protein. Apocytochrome *c* binding to phosphatidylserine dispersions decreases with increasing salt concentration from a saturation value corresponding to approximately 5 lipids per protein in the absence of salt to practically zero at 0.4 M NaCl. The perturbation of the spin-label mobility exhibits a parallel dependence on salt concentration. Binding of apocytochrome *c* to dimyristoylphosphatidylglycerol dispersions remains constant between pH 8 and pH 5.5, but then the number of lipids per protein bound increases by a factor of 2 on further decrease to pH 4. The overall spin-label mobility is little affected over the range pH 10-5.5 and exhibits a slight increase at lower pH. The number of motionally restricted spin-labeled lipids remains constant down to pH 5.5 and then increases abruptly. A comparison of the relative effects of apocytochrome *c* and cytochrome *c* binding in the presence and absence of salt yields very similar results with dimyristoylphosphatidylglycerol and beef heart cardiolipin to those obtained with phosphatidylserine. In particular, the maximum binding at a particular salt concentration is greater for the precursor apocytochrome *c* than for the mature protein cytochrome *c*.

The majority of mitochondrial proteins are synthesized on free ribosomes in the form of precursors which are subsequently imported into the organelle by a posttranslational transport step (Hay et al., 1984). Depending on the final destination of the protein, either insertion or translocation across one or two membranes has to occur. During this process the precursor (apoprotein) is converted into the mature holoprotein.

Apocytochrome *c*, the heme-free precursor of cytochrome *c*, has been extensively used to study the molecular details of posttranslational protein transport. Both the apoprotein and

† A long-term fellowship from the Deutsche Forschungsgemeinschaft to H.G. and a short-term EMBO fellowship to A.R. are gratefully acknowledged.
‡ Present address: BASF AG, Abt. Kunststofflaboratorium, D-6700 Ludwigshafen, Federal Republic of Germany.

0006-2960/86/0425-2904$01.50/0